Geometry and symmetry in quantum Boltzmann machine

Hai-Jing Song,^{1,2} Tieling Song,¹ Qi-Kai He,^{1,2} Yang Liu,³ and D. L. Zhou^{1,2,*}

¹Institute of Physics, Beijing National Laboratory for Condensed Matter Physics,

Chinese Academy of Sciences, Beijing 100190, China

²School of Physical Sciences, University of Chinese

Academy of Sciences, Beijing 100049, China

³QuantaEye Technologies Co., Ltd, Beijing 100083, China</sup>

Abstract

Quantum Boltzmann machine extends the classical Boltzmann machine learning to the quantum regime, which makes its power to simulate the quantum states beyond the classical probability distributions. We develop the BFGS algorithm to study the corresponding optimization problem in quantum Boltzmann machine, especially focus on the target states being a family of states with parameters. As an typical example, we study the target states being the real symmetric two-qubit pure states, and we find two obvious features shown in the numerical results on the minimal quantum relative entropy: First, the minimal quantum relative entropy in the first and the third quadrants is zero; Second, the minimal quantum relative entropy is symmetric with the axes y = x and y = -x even with one qubit hidden layer. Then we theoretically prove these two features from the geometric viewpoint and the symmetry analysis. Our studies show that the traditional physical tools can be used to help us to understand some interesting results from quantum Boltzmann machine learning.

 $^{^*}$ zhoudl
72@iphy.ac.cn

I. INTRODUCTION

The central aim of machine learning is to implement a task by building a mathematical model that simulates the learning processes of a human being with a computer [1–3]. One of the probabilistic machine learning models is the restricted Boltzmann machine [4, 5], which has been successfully used as a deep machine learning model in diverse tasks [6–8].

Recently in Ref. [9] M. H. Amin et al. proposed the quantum version of Boltzmann machine with a transverse field Ising Hamiltonian, and presented a training algorithm by sampling. In particular, they discussed the possibility of the implementation of such a Boltzmann machine in quantum annealing processors [10–12] like D-wave.

The main advantage of quantum Boltzmann machine is that it can simulate a multipartite entangled quantum state, which is beyond the classical probability distribution as shown in Bell's inequality [13–15]. According to modern physics, nature is governed by quantum mechanics, so it is necessary to extend the machine learning to the quantum regime.

The central problem in training Boltzmann machine is to minimize the quantum relative entropy [16] for the target state with respect to the states corresponding to the Boltzmann distributions for a given type of Hamiltonians [17]. We solve this minimization problem by adopting the BFGS algorithm [18, 19], where a recenter technique is adopted to increase the stability of our algorithm.

It is worth pointing out that the problem of minimizing the quantum relative entropy for the target state and the states of Boltzmann distributions is also explored in measuring the correlations of an *n*-partite quantum state in Refs. [20, 21]. Remarkably, the algorithms of calculating the many-body correlation were proposed in [22–24], which are applicable in quantum Boltzmann machine without hidden layers.

As a typical application of the above BFGS algorithm, we calculate the minimum quantum relative entropy for the target states being a family of two-qubit states with two real parameters, a radius and an angle. The minimal quantum relative entropy shows two obvious features: strongly angle-dependent and symmetric with two axes.

In general, numerical results from machine learning are hard to understand since the machine learning focuses on to dig out the results but not to discover the underlying mechanism. Therefore it is of great importance to grasp the underlying mechanism of the numerical optimal results [25]. To understand the above two features in the numerical results, here we

use a geometric method and a symmetry analysis to analytically explains these features.

Here we emphasize the relation between the learning problem and the optimization problem in quantum Boltzmann machine. In general, in a learning problem, only the learning sample is used to optimization, which is often a partial information for the target state; however, in our optimization problem, we assume that the target state is completely known, and our task is to adjust the parameters to get the approximate state as good as possible. In other words, the optimization problem gives the optimal capacity for the best approximate state for the learning problem in quantum Boltzmann machine [26, 27].

II. DEFINITION OF QUANTUM BOLTZMANN MACHINE

A quantum Boltzmann machine is composed by a bipartite quantum system, where one subsystem is called visible, and the other is called hidden [9]. The quantum state of the bipartite system is a Boltzmann thermal equilibrium state for a specific type Hamiltonian with variable parameters. The task of the quantum Boltzmann machine is to make the quantum state of the visible subsystem approximate a given target state as well as possible by adjusting the parameters in the Hamiltonian.

We formulate the Boltzmann machine mathematically as follows. Let $\mathcal{H}_v \otimes \mathcal{H}_h$ denote the product bipartite Hilbert space. The target state σ_* is defined on \mathcal{H}_v . A quantum Boltzmann machine has a specific type of Hamiltonians with parameters

$$H(\mathbf{a}) = -\mathbf{a} \cdot \mathbf{O},\tag{1}$$

where \mathbf{a} is the vector of real parameters, and \mathbf{O} is the vector of linearly independent Hermitian operators with zero trace. The quantum state of the bipartite quantum system is the Boltzmann thermal equilibrium state [22]

$$\rho(\mathbf{a}) = \frac{e^{-H(\mathbf{a})}}{\operatorname{Tr}(e^{-H(\mathbf{a})})} = \frac{e^{\mathbf{a} \cdot \mathbf{O}}}{\operatorname{Tr}(e^{\mathbf{a} \cdot \mathbf{O}})}.$$
 (2)

Then the reduced state of the visible subsystem is

$$\sigma(\mathbf{a}) = \operatorname{Tr}_h(\rho(\mathbf{a})), \tag{3}$$

where Tr_h denotes the trace over the hidden subsystem. The aim of the quantum Boltzmann machine is to minimize

$$S_m(\sigma_*) = \min_{\mathbf{a}} S(\sigma_* | \sigma(\mathbf{a})), \tag{4}$$

where the quantum relative entropy is defined as

$$S(\sigma|\sigma') = \text{Tr}_{v}(\sigma(\ln \sigma - \ln \sigma')). \tag{5}$$

Here the quantum relative entropy is used as a measure of the degree of approximation of one quantum state with another [20, 28].

III. BFGS ALGORITHM

In this section, we apply the Broyden-Fletcher-Goldfarb-Shanno (BFGS) algorithm to solve the minimization problem specified by Eq. (4).

The basic idea of the BFGS algorithm is as follows. The BFGS algorithm is iterative. First, choose an initial parameter vector \mathbf{a}^0 . In the (k+1)-th iteration, calculate \mathbf{a}^{k+1} from \mathbf{a}^k , which is realized in two steps. In the first step, find out the direction from \mathbf{a}^k to \mathbf{a}^{k+1} , which is determined by the second order Taylor expansion of the quantum relative entropy at the point \mathbf{a}_k :

$$S_q(\sigma_*|\sigma(\mathbf{a})) = S(\sigma_*|\sigma(\mathbf{a}^k)) + \mathbf{g}^{k\mathbf{T}}\mathbf{d}^k + \frac{1}{2}\mathbf{d}^{k\mathbf{T}}H^k\mathbf{d}^k,$$
(6)

where the upper index T denotes the transpose operation, and

$$\mathbf{d}^k = \mathbf{a} - \mathbf{a}^k,\tag{7}$$

$$\mathbf{g}^{k} = \left. \frac{\partial S(\sigma_{*} | \sigma(\mathbf{a}))}{\partial \mathbf{a}} \right|_{\mathbf{a}^{k}},\tag{8}$$

$$H^{k} = \frac{\partial^{2} S(\sigma_{*} | \sigma(\mathbf{a}_{k}))}{\partial \mathbf{a}^{k} \partial \mathbf{a}^{kT}} \bigg|_{\mathbf{a}^{k}}.$$
 (9)

If the Hessian matrix H^k is symmetric and positive, then $S_q(\sigma_*|\sigma(\mathbf{a}))$ in Eq. (6) has a minimum where the parameter vector \mathbf{a}_q^k satisfies

$$\mathbf{d}_{q}^{k} = \mathbf{a}_{q}^{k} - \mathbf{a}^{k} = -(H^{k})^{-1} \mathbf{g}^{k}. \tag{10}$$

In the second step, let

$$\mathbf{a}^{k+1} - \mathbf{a}^k = -\lambda^k (H^k)^{-1} \mathbf{g}^k. \tag{11}$$

Then use the line search algorithm to determine λ^k by minimizing

$$\min_{\lambda^k} S(\sigma_* | \sigma(\mathbf{a}^k - \lambda^k (H^k)^{-1} \mathbf{g}^k)). \tag{12}$$

The key element in the BFGS algorithm is to derive iteratively $(H^k)^{-1}$ from \mathbf{d}^k and \mathbf{g}^k , which is explained in Ref. [29].

As discussed above, it is helpful to get the analytical expression of the first derivative of $S(\sigma_*|\sigma(\mathbf{a}))$. Let us start the calculations with the case without the hidden subsystem. In this case, the first order derivative is

$$\frac{\partial S(\sigma_* | \sigma(\mathbf{a}))}{\partial a_i} = -\operatorname{Tr}\left(\sigma_* \frac{\partial}{\partial a_i} \ln \frac{e^{\mathbf{a} \cdot \mathbf{O}}}{\operatorname{Tr}(e^{\mathbf{a} \cdot \mathbf{O}})}\right)$$

$$= -\operatorname{Tr}\left(\sigma_* \frac{\partial}{\partial a_i} \left(\mathbf{a} \cdot \mathbf{O} - \operatorname{Tr}\left(e^{\mathbf{a} \cdot \mathbf{O}}\right)\right)\right)$$

$$= -\operatorname{Tr}(\sigma_* O_i) + \frac{\operatorname{Tr}\left(O_i e^{\mathbf{a} \cdot \mathbf{O}}\right)}{\operatorname{Tr}\left(e^{\mathbf{a} \cdot \mathbf{O}}\right)}$$

$$= \operatorname{Tr}(\rho(\mathbf{a})O_i) - \operatorname{Tr}(\sigma_* O_i). \tag{13}$$

The parameter vector \mathbf{a}_* satisfies

$$Tr(\rho(\mathbf{a})O_i) = Tr(\sigma_*O_i). \tag{14}$$

In other words, we only need to find the minimization of Eq. (4) in the set of states given by Eq. (14). In fact, the parameter vector \mathbf{a}_* can be determined by

$$\max_{\mathbf{a}} S(\rho(\mathbf{a})),\tag{15}$$

where a satisfies Eq. (14), and the Von Neumann entropy $S(\tau) = -\operatorname{Tr}(\tau \ln \tau)$. In this case

$$S(\sigma_*|\rho(\mathbf{a}_*)) = \operatorname{Tr}(\sigma_* \ln \sigma_*) - \operatorname{Tr}(\sigma_* \ln(\rho(\mathbf{a}_*)))$$

$$= \operatorname{Tr}(\sigma_* \ln \sigma_*) - \operatorname{Tr}(\sigma_*(\mathbf{a}_* \cdot \mathbf{O} - \ln(\operatorname{Tr}(e^{\mathbf{a}_* \cdot \mathbf{O}}))))$$

$$= \operatorname{Tr}(\sigma_* \ln \sigma_*) - \operatorname{Tr}(\rho(\mathbf{a}_*)(\mathbf{a}_* \cdot \mathbf{O} - \ln(\operatorname{Tr}(e^{\mathbf{a}_* \cdot \mathbf{O}}))))$$

$$= S(\rho(\mathbf{a}_*)) - S(\sigma_*). \tag{16}$$

Now let us consider the Boltzmann machine with a hidden subsystem. Then the first derivative of $S(\sigma_*, \sigma(\mathbf{a}))$ is

$$\frac{\partial S(\sigma_* | \sigma(\mathbf{a}))}{\partial a_i} = -\frac{\partial}{\partial a_i} \operatorname{Tr}_v \left(\sigma_* \ln \frac{\operatorname{Tr}_h \left(e^{\mathbf{a} \cdot \mathbf{O}} \right)}{\operatorname{Tr} \left(e^{\mathbf{a} \cdot \mathbf{O}} \right)} \right)
= -\operatorname{Tr}_v \left(\sigma_* \frac{\partial}{\partial a_i} \ln \frac{\operatorname{Tr}_h \left(e^{\mathbf{a} \cdot \mathbf{O}} \right)}{\operatorname{Tr} \left(e^{\mathbf{a} \cdot \mathbf{O}} \right)} \right)
= -\operatorname{Tr}_v \left(\sigma_* \frac{\partial}{\partial a_i} \ln \operatorname{Tr}_h \left(e^{\mathbf{a} \cdot \mathbf{O}} \right) \right) + \frac{\partial}{\partial a_i} \ln \operatorname{Tr} \left(e^{\mathbf{a} \cdot \mathbf{O}} \right)
= \operatorname{Tr}(\rho(\mathbf{a}) O_i) - \operatorname{Tr}_v \left(\sigma_* \frac{\partial}{\partial a_i} \ln \operatorname{Tr}_h \left(e^{\mathbf{a} \cdot \mathbf{O}} \right) \right).$$
(17)

In Section 3.3 of [30] Hiai Fumio and Petz Dnes give a convenient formula for the derivation (with respect to $t \in R$):

$$\frac{d}{dt}\log(A+tT) = \int_0^\infty dx (xI+A)^{-1} T(xI+A)^{-1}.$$
 (18)

Let

$$E(\mathbf{a}) = e^{\mathbf{a} \cdot \mathbf{O}} = \sum_{l} e_{l} |l\rangle\langle l|, \tag{19}$$

$$D(\mathbf{a}) = \operatorname{Tr}_h(E(\mathbf{a})) = \sum_{x} |x\rangle d_x \langle x|, \qquad (20)$$

$$B_i(\mathbf{a}) = \frac{\partial D(\mathbf{a})}{\partial a_i}. (21)$$

Then we have

$$\frac{\partial S(\sigma_*|\rho(\mathbf{a}))}{\partial a_i} = \text{Tr}(\rho(\mathbf{a})O_i) - \int_0^\infty ds \, \text{Tr}_v \left(\sigma_* \frac{1}{D+s} B_i \frac{1}{D+s}\right),\tag{22}$$

where the integral

$$\int_{0}^{\infty} ds \operatorname{Tr}_{v} \left(\sigma_{*} \frac{1}{D+s} B_{i} \frac{1}{D+s} \right)
= \sum_{x,y} \int_{0}^{\infty} ds \frac{1}{d_{x}+s} \frac{1}{d_{y}+s} \operatorname{Tr}_{v} \left(\sigma_{*} | x \rangle \langle x | B_{i} | y \rangle \langle y | \right)
= \sum_{x,y} \frac{\ln d_{y} - \ln d_{x}}{d_{y} - d_{x}} \langle y | \sigma_{*} | x \rangle \langle x | B_{i} | y \rangle$$
(23)

with

$$B_{i}(\mathbf{a}) = \frac{\partial D(\mathbf{a})}{\partial a_{i}}$$

$$= \operatorname{Tr}_{h} \left(\int_{0}^{1} d\tau e^{\tau \mathbf{a} \cdot \mathbf{O}} O_{i} e^{(1-\tau)\mathbf{a} \cdot \mathbf{O}} \right)$$

$$= \sum_{l,m} \operatorname{Tr}_{h} \left(\int_{0}^{1} d\tau e^{\tau}_{l} e^{1-\tau}_{m} |l\rangle \langle l| O_{i} |m\rangle \langle m| \right)$$

$$= \sum_{l,m} \operatorname{Tr}_{h} \left(\frac{e_{l} - e_{m}}{\ln e_{l} - \ln e_{m}} |l\rangle \langle l| O_{i} |m\rangle \langle m| \right). \tag{24}$$

Here we take the limit to deal with the cases of $d_y = d_x$ and $e_l = e_m$:

$$\lim_{d_y \to d_x} \frac{\ln d_y - \ln d_x}{d_y - d_x} = \frac{1}{d_x},\tag{25}$$

$$\lim_{e_m \to e_l} \frac{e_l - e_m}{\ln e_l - \ln e_m} = e_l. \tag{26}$$

Since the above expression of the first order derivative of the quantum relative entropy does not contain derivatives or integrals, its numerical calculation becomes more effective and more accurate, which significantly enhances the performance of the BFGS algorithm.

IV. GEOMETRY IN QUANTUM BOLTZMANN MACHINE WITHOUT HIDDEN SUBSYSTEM

Let us start from the quantum Boltzmann machine without the hidden subsystem, and the visible subsystem composed by two qubits. The Hamiltonian is given by [31]

$$H = -\sum_{i=1}^{2} a_i X_i - \sum_{i=1}^{2} a_{i+2} Z_i - a_5 Z_1 \otimes Z_2, \tag{27}$$

where X and Z are two Pauli matrices. The eigen problem of Z is given by $Z|n\rangle = (-1)^n|n\rangle$ with $n \in \{0, 1\}$, and the operator X is defined by $X|n\rangle = |1 - n\rangle$.

To be concrete, the target states we study are the following set of symmetric pure states

$$|\psi(r,\phi)\rangle = \sqrt{1-r^2} \frac{|01\rangle + |10\rangle}{\sqrt{2}} + r\cos\phi|00\rangle + r\sin\phi|11\rangle, \tag{28}$$

where $r \in [0, 1]$ and $\phi \in [0, 2\pi]$.

First, we numerically investigate the problem based on the BFGS algorithm. The numerical result of the minimum quantum relative entropy for the states $|\psi(r,\phi)\rangle$ is shown in Fig. 1.

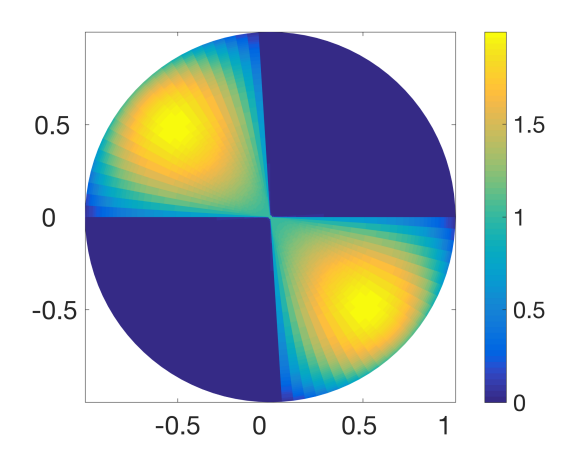


FIG. 1: The minimum relative entropy for the states $|\psi(r,\phi)\rangle$. Here the coordinates r,ϕ are the polar coordinates. The minimum relative entropy is represented by the colors.

We find the following four features of the numerical results from the numerical results.

1. When the coordinates (r, ϕ) are in the first quadrant and in the third quadrant, the minimum relative entropy of the states $|\psi(r, \phi)\rangle$ to the exponential state family specified by H are zero, i.e.

$$S_m(r,\phi) = 0, \text{ if } 0 < r < 1 \text{ and } \phi \in (0, \frac{\pi}{2}) \text{ or } \phi \in (\pi, \frac{3\pi}{2}),$$
 (29)

which implies that every state in these two regions can be represented by one of the exponential states perfectly.

2. When r=1, the minimum quantum relative entropy $S_m(1,\phi)$ is periodic

$$S_m(1, \phi + \frac{\pi}{2}) = S_m(1, \phi),$$
 (30)

$$S_m(1,0) = 0, (31)$$

$$S_m(1, \frac{\pi}{4}) = 1. (32)$$

- 3. When r=0, the minimal quantum relative entropy $S_m(0,\phi)=1$.
- 4. In addition, the maximal minimal quantum relative entropy is 2, which appears at two states:

$$S_m\left(\frac{\sqrt{2}}{2}, \frac{3\pi}{4}\right) = S_m\left(\frac{\sqrt{2}}{2}, \frac{7\pi}{4}\right) = 2.$$
 (33)

Why the minimum quantum relative entropy for the states $|\psi(r,\phi)\rangle$ in the first quadrant and the third quadrant are zeros, but they are nonzero for the states in the second and the fourth quadrant?

To make the quantum relative entropy become zero, there must exist a Hamiltonian H in Eq. (27) such that

$$|\psi(r,\phi)\rangle\langle\psi(r,\phi)| = \frac{e^H}{\text{Tr}(e^H)}.$$
 (34)

The above equation seems to give the following paradox: the left side is a pure state, while the right side is a mixed state, and the equality can not be satisfied. This paradox can be solved as follows. Since the state in the right hand side can be imagined as the thermal equilibrium state of a Hamiltonian H' at temperature T with the relation

$$H = -\frac{1}{k_B T} H',\tag{35}$$

where k_B is the Boltzmann constant. When H' has a unique ground state, the thermoequilibrium state will limit to the ground state at the zero temperature. Thus, to prove the characteristic of the minimum quantum relative entropy in Eq. (29), we need to prove there exist a H' with $|\psi(r,\phi)\rangle$ in the first and the third quadrant being the unique ground state, and there does not exist such a H' for $|\psi(r,\phi)\rangle$ in the second and the fourth quadrant.

For the quantum Boltzmann without hidden layers, we may show that there is a unique H such that the minimum quantum relative entropy is arrived at. Since the target state $|\psi(r,\phi)\rangle$ is symmetric for the permutation of qubit 1 and qubit 2, the corresponding Hamiltonian must be symmetric with respect to the permutation. Without losing of generality, we assume that the Hamiltonian

$$H' = a(Z_1 + Z_2) + b(X_1 + X_2) + Z_1 \otimes Z_2, \tag{36}$$

namely, $a_1 = a_2 = b$, $a_3 = a_4 = a$, and $a_5 = 1$. The average energy for the state $|\psi(r,\phi)\rangle$ is

$$E(a,b;r,\phi) = \langle \psi(r,\phi)|H'|\psi(r,\phi)\rangle$$

= $2ar^2\cos 2\phi + 4br\sqrt{1-r^2}\sin\left(\phi + \frac{\pi}{4}\right) + 2r^2 - 1.$ (37)

The necessary condition for (r, ϕ) being an extreme point is

$$\frac{\partial E(a,b;r,\phi)}{\partial r} = 4ar\cos 2\phi + 4b\sin(\phi + \frac{\pi}{4})\frac{1 - 2r^2}{\sqrt{1 - r^2}} + 4r = 0,$$
 (38)

$$\frac{\partial E(a,b;r,\phi)}{\partial \phi} = -4ar^2 \sin 2\phi + 4br\sqrt{1-r^2} \cos\left(\phi + \frac{\pi}{4}\right) = 0. \tag{39}$$

Thus we get

$$a_* = -\frac{(1 - r^2)\cot(\phi + \frac{\pi}{4})}{1 - 2r^2\sin^2(\phi + \frac{\pi}{4})},\tag{40}$$

$$b_* = -\frac{r\sqrt{1 - r^2}\sin 2\phi \csc(\phi + \frac{\pi}{4})}{1 - 2r^2\sin^2(\phi + \frac{\pi}{4})}.$$
 (41)

The Hessian matrix [32]

$$H = \begin{pmatrix} \frac{\partial^{2} E(a,b;r,\phi)}{\partial r^{2}} & \frac{\partial^{2} E(a,b;r,\phi)}{\partial r \partial \phi} \\ \frac{\partial^{2} E(a,b;r,\phi)}{\partial \phi \partial r} & \frac{\partial^{2} E(a,b;r,\phi)}{\partial r^{2}} \end{pmatrix}$$

$$= \begin{pmatrix} 4a\cos 2\phi + \frac{4br\sin(\phi + \frac{\pi}{4})(2r^{2} - 3)}{(1 - r^{2})^{3/2}} + 4 & -8ar\sin 2\phi + 4b\cos(\phi + \frac{\pi}{4})\frac{1 - 2r^{2}}{\sqrt{1 - r^{2}}} \\ -8ar\sin 2\phi + 4b\cos(\phi + \frac{\pi}{4})\frac{1 - 2r^{2}}{\sqrt{1 - r^{2}}} & -8ar^{2}\cos 2\phi - 4br\sqrt{1 - r^{2}}\sin(\phi + \frac{\pi}{4}) \end{pmatrix}$$
(42)

Then the Hessian matrix at the extreme point (a_*, b_*)

$$H_{a_*,b_*} = \begin{pmatrix} \frac{4\sin 2\phi}{(1-r^2)(1-r^2(1+\sin 2\phi))} & \frac{4r\sin 2\phi\cot\left(\phi + \frac{\pi}{4}\right)}{1-r^2(1+\sin 2\phi)} \\ \frac{4r\sin 2\phi\cot\left(\phi + \frac{\pi}{4}\right)}{1-r^2(1+\sin 2\phi)} & \frac{4r^2(1-r^2)(2-\sin 2\phi)}{1-r^2(1+\sin 2\phi)} \end{pmatrix}$$
(43)

The determinant

$$Det(H_{a_*,b_*}) = \frac{32r^2 \sin 2\phi}{(1+\sin 2\phi)(1-r^2(1+\sin 2\phi))^2}.$$
 (44)

When $\operatorname{Det}(H_{a_*,b_*}) > 0$, i.e. $\phi \in (0, \frac{\pi}{2})$ or $\phi \in (\pi, \frac{3\pi}{2})$, the Hamiltonian H_{a_*,b_*} is positive or negative, and $E(a_*,b_*;r,\phi)$ is the local minimum or maximum. In addition, when $\phi \in (\frac{\pi}{2},\pi)$ or $\phi \in (\frac{3\pi}{2},2\pi)$, $\operatorname{Det}(H_{a_*,b_*}) < 0$, which implies that $E(a_*,b_*;r,\phi)$ is a saddle point. Thus for $|\psi(r,\phi)\rangle$ in the first and the third quadrant there exists a Hamiltonian H' (or -H') in Eq. (36) with the state as its unique ground state. However, for $|\psi(r,\phi)\rangle$ in the second and the fourth quadrant there does not exist such a Hamiltonian H.

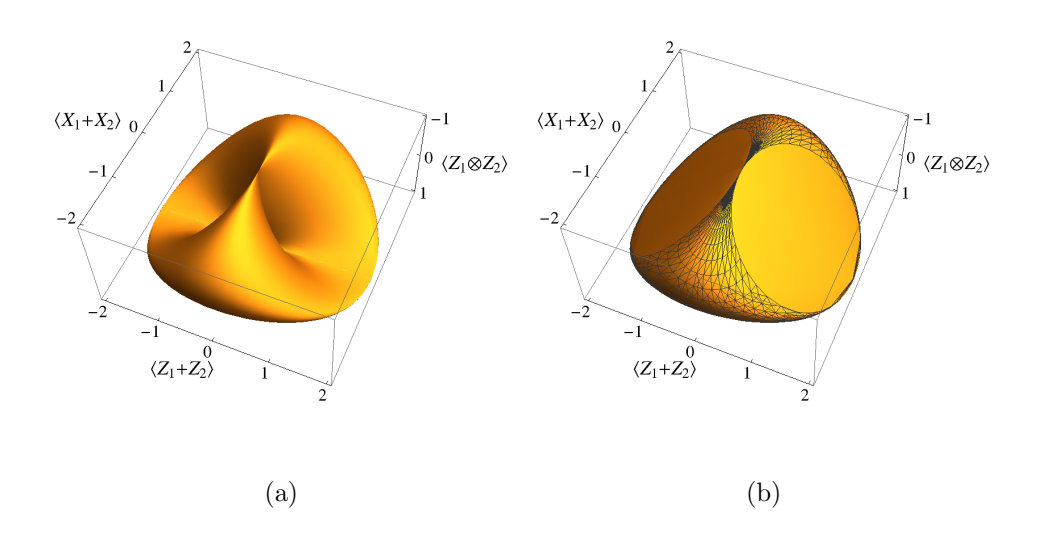


FIG. 2: The numerical range of the Hermitian operators $\{Z_1 + Z_2, X_1 + X_2, Z_1 \otimes Z_2\}$ and the black net lines corresponding to the states $|\psi(r,\phi)\rangle$ in the first and the third quadrants.

The above analysis can be clearly demonstrated in the geometric pictures shown in Fig. 2 [33–35]. The average values of the Hermitian operators $\{Z_1 + Z_2, X_1 + X_2, Z_1 \otimes Z_2\}$ for the states $|\psi(r,\phi)\rangle$ are plotted as a closed surface in Fig. 2 (a), and the average values of the same three operators are plotted as a convex body shown in Fig. 2 (b). In particular, for the states $|\psi(r,\phi)\rangle$ in the first and the third quadrant, the corresponding points lie in the surface of the numerical range, as shown by the black network in Fig. 2 (b). For the states $|\psi(r,\phi)\rangle$ in the second and the fourth quadrant, the corresponding points enter the interior of the convex body.

Note that the Hamiltonian in Eq. (36) and a constant e defines a hyperplane specified by

$$a\langle Z_1 + Z_2 \rangle + b\langle X_1 + X_2 \rangle + \langle Z_1 \otimes Z_2 \rangle = e. \tag{45}$$

At any point corresponding to the state $|\psi(r,\phi)\rangle$ in the first or the third quadrant, there is a unique hyperplane specified by constants a,b and e tangent with the convex body [36]. The constants a,b define the Hamiltonian H' or -H' with $|\psi(r,\phi)\rangle$ as its unique ground state. Hence we show that the minimum quantum relative entropy is zero for the state $|\psi(r,\phi)\rangle$ in the first and third quadrant. For the state $|\psi(r,\phi)\rangle$ in the second and fourth quadrant lying in the interior of the convex body, there is no such a tangent hyperplane, and thus the minimal quantum relative entropy becomes nonzero.

Let us consider the states $|\psi(1,\phi)\rangle$. The average values

$$\langle \psi(1,\phi)|X_1 + X_2|\psi(1,\phi)\rangle = 0, \tag{46}$$

$$\langle \psi(1,\phi)|Z_1 + Z_2|\psi(1,\phi)\rangle = 2\cos(2\phi),\tag{47}$$

$$\langle \psi(1,\phi)|Z_1 \otimes Z_2|\psi(1,\phi)\rangle = 1. \tag{48}$$

Then all the two-qubit states that satisfy the above conditions can be written as

$$\tau = \frac{I}{4} + \cos(2\phi) \frac{Z_1 + Z_2}{4} + \frac{Z_1 \otimes Z_2}{4} + \dots$$
 (49)

In terms of the basis specified the common eigenstates of Z_1 and Z_2 , the diagonal state

$$\operatorname{diag}(\tau) = \frac{I}{4} + \cos(2\phi) \frac{Z_1 + Z_2}{4} + \frac{Z_1 \otimes Z_2}{4}.$$
 (50)

Because the Von Neaumann entropy for any quantum state is not more than that of its diagonal state. According to Theorem 11.9 of Section 11.3.3 in [37], we have

$$S(\tau) \le S(\operatorname{diag}(\tau)).$$
 (51)

Thus the minimal quantum relative entropy is

$$S_m(1,\phi) = S(\operatorname{diag}(\tau)) = -\cos^2\phi \ln(\cos^2\phi) - \sin^2\phi \ln(\sin^2\phi). \tag{52}$$

The analytical result in Eq. (52) is demonstrated in Fig. 3 (a), together with the numerical result. These two results from the BFGS algorithm agree well with each other.

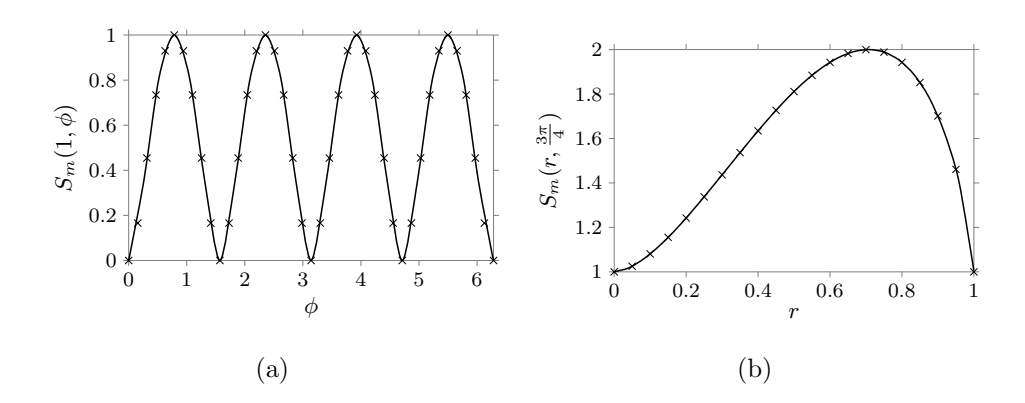


FIG. 3: The minimal quantum relative entropy in the two cases: (a) r = 1; (b) $\phi = \frac{3\pi}{4}$. The analytical results are plotted as the solid lines, and the numerical results are plotted as cross marks.

Now we consider the states $|\psi(r,\frac{3\pi}{4})\rangle$. The average values

$$\left\langle \psi(r, \frac{3\pi}{4}) \middle| X_1 + X_2 \middle| \psi(r, \frac{3\pi}{4}) \right\rangle = 0, \tag{53}$$

$$\left\langle \psi(1, \frac{3\pi}{4}) \middle| Z_1 + Z_2 \middle| \psi(1, \frac{3\pi}{4}) \right\rangle = 0,$$
 (54)

$$\left\langle \psi(1, \frac{3\pi}{4}) \middle| Z_1 \otimes Z_2 \middle| \psi(1, \frac{3\pi}{4}) \right\rangle = 2r^2 - 1.$$
 (55)

Then all the two-qubit states that satisfy the above conditions can be written as

$$\tau = \frac{I}{4} + (2r^2 - 1)\frac{Z_1 \otimes Z_2}{4} + \dots$$
 (56)

In terms of the basis specified the common eigenstates of Z_1 and Z_2 , the diagonal state

$$\operatorname{diag}(\tau) = \frac{I}{4} + (2r^2 - 1)\frac{Z_1 \otimes Z_2}{4}.$$
 (57)

Because the Von Neaumann entropy for any quantum state is not more than that of its diagonal state. According to Theorem 11.9 of Section 11.3.3 in [37], we have

$$S(\tau) \le S(\operatorname{diag}(\tau)).$$
 (58)

Thus the minimal quantum relative entropy is

$$S_m(r, \frac{3\pi}{4}) = S(\operatorname{diag}(\tau)) = -r^2 \ln r^2 - (1 - r^2) \ln(1 - r^2) + 1, \tag{59}$$

which is demonstrated in Fig. 3 (b) supported by the numerical results from the BFGS algorithm.

V. SYMMETRY IN QUANTUM BOLTZMAN MACHINE

In this section, we will explore to investigate the power of the hidden subsystem in improving the capacity of the quantum Boltzmann machine. More precisely, we study a three-qubit system with the third qubit being the hidden subsystem, whose Hamiltonian is

$$H = -\sum_{i=1}^{3} a_i X_i - \sum_{i=1}^{3} a_{i+3} Z_i - a_7 Z_2 \otimes Z_3 - a_8 Z_1 \otimes Z_3 - a_9 Z_1 \otimes Z_2.$$
 (60)

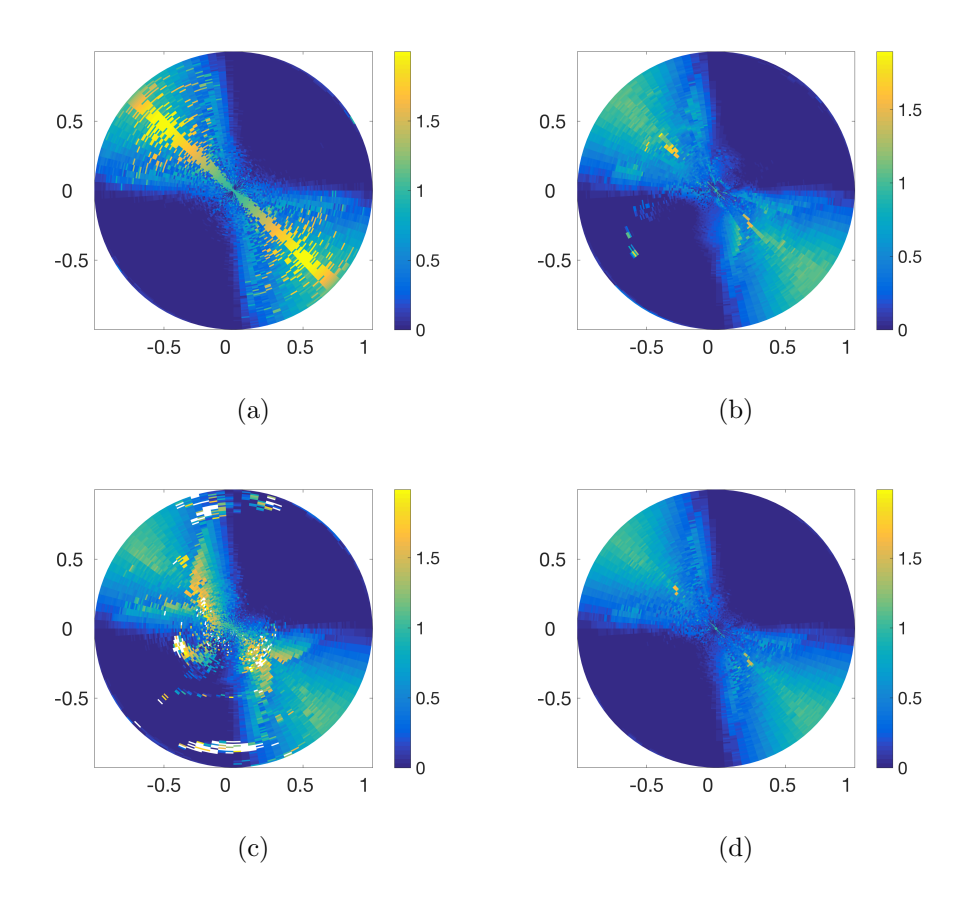


FIG. 4: The minimal quantum relative entropy for different initial conditions. (a) $\mathbf{a} = 0$. (b) $\mathbf{a} = 1$. (c) $\mathbf{a} = 2$, and the white color denote the calculated minimal quantum relative entropy is larger than 2 at the point. (d) The minimum quantum relative entropy taken over the cases (a), (b), and (c).

We still study the target states $|\psi(r,\phi)\rangle$ in Eq. (28). The numerical results from the BFGS algorithm are shown in Fig. 4, where the results for different initial parameters $\mathbf{a} = 0$, $\mathbf{a} = 1$, and $\mathbf{a} = 2$ are shown in Fig. 4 (a), (b), and (c) respectively. Obviously, when the hidden subsystem, the third qubit, is involved, the relative entropy will have many local

minimums, rather than only one minimum in the case without hidden subsystems. The minimal quantum relative entropy taken over the cases (a), (b), (c) is shown in Fig. 4 (d). Compared the results in Fig. 4 (d) and Fig. 1, we observe that the relative entropy decreases obviously, e.g. the maximal minimum quantum relative entropy at $\{r = \sqrt{2}/2, \phi = \frac{3\pi}{4}\}$ decreases from 2 to about 1.00.

The numerical results in Fig. 4 (d) and Fig. 1 show that there are two symmetric axes: y = x and y = -x in the minimal quantum relative entropy of $|\psi(r, \phi)\rangle$. Now let us analyze the symmetry in the quantum Boltzmann machine for the target states $\sigma_*(\mathbf{r})$.

First, we notice that the local unitary transformation U_v simultaneously acting on $\sigma_*(\mathbf{r})$ and $\sigma(\mathbf{a})$ does not change the quantum relative entropy, i.e.,

$$S(U_v \sigma_*(\mathbf{r}) U_v^{\dagger} | U_v \sigma(\mathbf{a}) U_v^{\dagger}) = S(\sigma_*(\mathbf{r}) | \sigma(\mathbf{a})). \tag{61}$$

In addition, a local unitary transformation U_h acting on the hidden subsystem does not change the reduced state $\sigma(\mathbf{a})$. In other words, the quantum relative entropy $S(\sigma_*(\mathbf{r})|\sigma(\mathbf{a}))$ is invariant under arbitrary unitary transformation $U_v \otimes U_h$.

To make the unitary transformation $U_v \otimes U_h$ become a symmetric operation, we require that

$$U_v \sigma_*(\mathbf{r}) U_v^{\dagger} = \sigma_*(\mathbf{r}'), \tag{62}$$

$$U_v \otimes U_h H(\mathbf{a}) U_h^{\dagger} \otimes U_v^{\dagger} = H(\mathbf{a}'),$$
 (63)

where $H(\mathbf{a})$ is the Hamiltonian in Eq. (1). In other words, we require that the unitary transformation keeps the forms of $\sigma_*(\mathbf{r})$ and $H(\mathbf{a})$, and it only changes the parameters from $\{\mathbf{r}, \mathbf{a}\}$ to $\{\mathbf{r}', \mathbf{a}'\}$.

As an example, we will show that $U_v = X_1 \otimes X_2$ and $U_h = I_3$ is a symmetric operation. Note that

$$|\psi(r, \frac{\pi}{2} - \phi)\rangle = X_1 \otimes X_2 |\psi(r, \phi)\rangle,$$
 (64)

and

$$H(\mathbf{a}') = X_1 \otimes X_2 H(\mathbf{a}) X_1 \otimes X_2 \tag{65}$$

$$= -\sum_{i=1}^{3} a_i X_i + \sum_{i=1}^{2} a_{i+3} Z_i - a_6 Z_3 - a_9 Z_1 \otimes Z_2 + a_7 Z_2 \otimes Z_3 + a_8 Z_1 \otimes Z_3,$$
 (66)

which gives the relation between \mathbf{a}' and \mathbf{a} . Thus we obtain

$$S(\sigma_*(r, \frac{\pi}{2} - \phi) | \sigma(\mathbf{a}')) = S(\sigma_*(r, \phi) | \sigma(\mathbf{a})). \tag{67}$$

Because the above relation is valid for arbitrary ϕ and **a**, we conclude that

$$\min_{\mathbf{a}'} S(\sigma_*(r, \frac{\pi}{2} - \phi) | \sigma(\mathbf{a}')) = \min_{\mathbf{a}} S(\sigma_*(r, \phi) | \sigma(\mathbf{a})), \tag{68}$$

i.e.,

$$S_m(r, \frac{\pi}{2} - \phi) = S_m(r, \phi). \tag{69}$$

Similarly, for the symmetric operation $U_v = Y_1 \otimes Y_2$ and $U_h = I_3$, we can show that

$$S_m(r, \frac{3\pi}{2} - \phi) = S_m(r, \phi).$$
 (70)

This implies that the states (r, ϕ) , $(r, \frac{\pi}{2} - \phi)$, $(r, \frac{3\pi}{2} - \phi)$ and $(r, \pi + \phi)$ has the same minimum quantum relative entropy. Because of the symmetry, we only need to consider the states for $\phi \in [\frac{\pi}{4}, \frac{3\pi}{4}]$.

In fact, up to a phase factor, all the symmetry operations can be written as

$$\{X_1 \otimes X_2, Y_1 \otimes Y_2, Z_1 \otimes Z_2, I_1 \otimes I_2\} \otimes \{X_3, Y_3, Z_3, I_3\}.$$
 (71)

Let us consider the symmetric operation $U_v = I_1 \otimes I_2$ and $U_h = X_3$. Then we have

$$S(\sigma_*(\mathbf{r})|\sigma(\mathbf{a}')) = S(\sigma_*(\mathbf{r})|\sigma(\mathbf{a}))$$
(72)

with

$$H(\mathbf{a}') = -\sum_{i=1}^{3} a_i X_i - \sum_{i=1}^{5} a_i Z_i - a_9 Z_1 \otimes Z_2 + a_6 Z_3 + a_8 Z_1 \otimes Z_3 + a_7 Z_2 \otimes Z_3.$$
 (73)

This implies that if **a** corresponds to a minimum, then **a**' must also be a minimum. If the hidden subsystem decrease $S_m(\mathbf{r})$, then $d_{13}d_{23} \neq 0$, which leads to $\mathbf{a}' \neq \mathbf{a}$, i.e., there are at least 2 degenerate parameter vectors **a** for the same state.

In general, when there is a hidden subsystem, there are many local minimums, which makes the numerical results from our BFGS algorithm strongly depends on the initial parameter vector \mathbf{a}_0 , and it is hard to obtain the global minimum. Here for each target state, we take the minimum from the numerical results with 1000 random initial parameter vectors \mathbf{a}_0 . The numerical results are shown in Fig. 5. For the states $|\psi(1,\phi)\rangle$, the hidden subsystem does not increase the power of the quantum Boltzmann machine. However, the hidden subsystem significantly increases the power of the quantum Boltzmann machine for the states $|\psi(r,\frac{3\pi}{4})\rangle$ with 0 < r < 1.

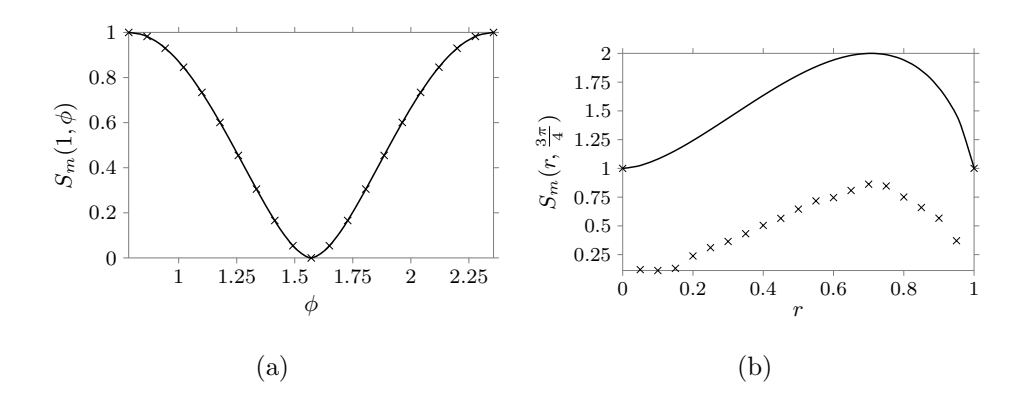


FIG. 5: The minimal quantum relative entropy in the two cases: (a) r = 1; (b) $\phi = \frac{3\pi}{4}$. The analytical results without the hidden subsystem are plotted as the solid lines, and the numerical results with the hidden subsystem are plotted as cross marks.

VI. DISCUSSION AND SUMMARY

We developed the optimization BFGS algorithm for quantum Boltzmann machine based on analytical results on the first order derivatives of quantum relative entropy. Then we apply the algorithm to the two-qubit target states, a family of states with two parameters with the transverse Ising model without or with hidden layers.

For the machine learning model without hidden layers, the numerical results show that the target states in the first and the third quadrants are perfectly represented by the Boltzmann machine, while the target states in the second and the fourth quadrants are not. We use the numerical range of related observables for any states forms a convex body, and we further show that the target states in the first and third quadrants lie in the surface of the convex body, but those states in the second and the fourth quadrants lie in the interior of the convex body. Since a Hamiltonian specifies a hyperplane in the case, the states in the surface can be regarded as the ground states of the Hamiltonian, which can be used to construct the Boltzman machine. Thus the geometric picture gives a clear physical explanation of the quadrant-dependent behavior of the minimum quantum relative entropy.

For the quantum Boltzmann machine with or without hidden layers, there are two symmetric axes: y = x and y = -x in the minimal quantum relative entropy of $|\psi(r,\phi)\rangle$. We clarify how to define the symmetric operation from the invariance of quantum relative entropy under local unitary transformations. Then we prove the symmetry in our problem by explicitly constructing the symmetric operations corresponding to these two symmetric

axes. Furthermore, we also use a symmetry argument to show that there are many local minimums for the Boltzmann machine with hidden layers.

In summary, we study a family of target states with the quantum Boltzmann machine by developing the BFGS algorithm, and explain the numerical results through the geometric method and the symmetry analysis. We hope that our results can lead to the global characterization on the target states, and increases the understanding of quantum machine learning [38–41].

ACKNOWLEDGMENTS

This work is supported by NSF of China (Grant Nos. 11475254 and 11775300), NKBRSF of China (Grant No. 2014CB921202), the National Key Research and Development Program of China (2016YFA0300603).

- [1] David E. Goldberg and John H. Holland. Genetic algorithms and machine learning. *Machine Learning*, 3(2):95–99, Oct 1988.
- [2] Christophe Andrieu, Nando de Freitas, Arnaud Doucet, and Michael I. Jordan. An introduction to mcmc for machine learning. *Machine Learning*, 50(1):5–43, Jan 2003.
- [3] M. I. Jordan and T. M. Mitchell. Machine learning: Trends, perspectives, and prospects. Science, 349(6245):255–260, 2015.
- [4] Nan Zhang, Shifei Ding, Jian Zhang, and Yu Xue. An overview on restricted boltzmann machines. *Neurocomputing*, 275:1186 1199, 2018.
- [5] Y. Nomura, A. S. Darmawan, Y. Yamaji, and M. Imada. Restricted Boltzmann machine learning for solving strongly correlated quantum systems. *Phys. Rev. B*, 96(20):205152, November 2017.
- [6] Simon Osindero Geoffrey E. Hinton and Yee-Whye Teh. A fast learning algorithm for deep belief nets. *Neural Computation*, 18:1527–1554, July 2006.
- [7] G. Carleo, Y. Nomura, and M. Imada. Constructing exact representations of quantum many-body systems with deep neural networks. *ArXiv e-prints*, February 2018.
- [8] Lok-Won Kim. DeepX: Deep Learning Accelerator for Restricted Boltzmann Machine Ar-

- tificial Neural Networks. *IEEE Transactions on Neural Networks and Learning Systems*, 29(5):1441–1453, May 2018.
- [9] Mohammad H. Amin, Evgeny Andriyash, Jason Rolfe, Bohdan Kulchytskyy, and Roger Melko. Quantum boltzmann machine. *Phys. Rev. X*, 8:021050, May 2018.
- [10] S. H. Adachi and M. P. Henderson. Application of Quantum Annealing to Training of Deep Neural Networks. ArXiv e-prints, October 2015.
- [11] Marcello Benedetti, John Realpe-Gómez, Rupak Biswas, and Alejandro Perdomo-Ortiz. Estimation of effective temperatures in quantum annealers for sampling applications: A case study with possible applications in deep learning. *Phys. Rev. A*, 94:022308, Aug 2016.
- [12] Sergio Boixo, Tameem Albash, Federico M. Spedalieri, Chancellor, and Daniel A. Lidar. Experimental signature of programmable quantum annealing. *Nature Communications*, 4, June 2013.
- [13] H. J Kappen. Learning quantum models from quantum or classical data. ArXiv e-prints, March 2018.
- [14] J. Adcock, E. Allen, M. Day, S. Frick, J. Hinchliff, M. Johnson, S. Morley-Short, S. Pallister, A. Price, and S. Stanisic. Advances in quantum machine learning. ArXiv e-prints, December 2015.
- [15] S. Lloyd, M. Mohseni, and P. Rebentrost. Quantum algorithms for supervised and unsupervised machine learning. *ArXiv e-prints*, July 2013.
- [16] J.-H. Sim and M. J. Han. Maximum Quantum Entropy Method. ArXiv e-prints, April 2018.
- [17] Nihal Yapage. Information geometrical study of quantum Boltzmann machines. PhD thesis, The University of Electro-Communications (UEC) Tokyo, Japan, 2008.
- [18] Y. Yang. A Globally and Superlinearly Convergent Modified BFGS Algorithm for Unconstrained Optimization. *ArXiv e-prints*, December 2012.
- [19] J. Guo and A. Lewis. BFGS convergence to nonsmooth minimizers of convex functions. ArXiv e-prints, March 2017.
- [20] D. L. Zhou. Irreducible multiparty correlations in quantum states without maximal rank. Phys. Rev. Lett., 101:180505, Oct 2008.
- [21] D. L. Zhou. Irreducible multiparty correlations can be created by local operations. Phys. Rev. A, 80:022113, Aug 2009.
- [22] Matthias Kleinmann S?nke Niekamp, Tobias Galla and Otfried Ghne. Computing complexity

- measures for quantum states based on exponential families. *Journal of Physics A: Mathematical and Theoretical*, 46(12):125301, 2013.
- [23] Zhou Duan-Lu. Efficient numerical algorithm on irreducible multiparty correlations. Communications in Theoretical Physics, 61(2):187, 2014.
- [24] Yang Liu, Bei Zeng, and D L Zhou. Irreducible many-body correlations in topologically ordered systems. *New Journal of Physics*, 18(2):023024, 2016.
- [25] J. Frdric Bonnans J. Charles Gilbert Claude Lemarchal Claudia A. Sagastizbal. Numerical Optimization. Springer, Berlin, Heidelberg, 2006.
- [26] Mária Kieferová and Nathan Wiebe. Tomography and generative training with quantum boltzmann machines. *Phys. Rev. A*, 96:062327, Dec 2017.
- [27] M. Schuld, I. Sinayskiy, and F. Petruccione. An introduction to quantum machine learning.

 Contemporary Physics, 56:172–185, April 2015.
- [28] J. Realpe-Gómez, M. Benedetti, R. Biswas, and A. Perdomo-Ortiz. Quantum-assisted learning of graphical models with arbitrary pairwise connectivity. In APS Meeting Abstracts, page A51.005, 2017.
- [29] Jorge Nocedal and Stephen J. Wright. Numerica Optimization. Springer, 2006.
- [30] Dnes Petz Fumio Hiai. Introduction to Matrix Analysis and Applications. Universitext.
- [31] Nihal Yapage and Hiroshi Nagaoka. An information geometrical approach to the mean-field approximation for quantum ising spin models. *Journal of Physics A: Mathematical and Theoretical*, 41(6):065005, 2008.
- [32] J. A. Nelder and R. Mead. A simplex method for function minimization. *The Computer Journal*, 7(4):308–313, 1965.
- [33] V. Zauner, D. Draxler, L. Vanderstraeten, J. Haegeman, and F. Verstraete. Symmetry Breaking and the Geometry of Reduced Density Matrices. *ArXiv e-prints*, December 2014.
- [34] Ji-Yao Chen, Zhengfeng Ji, Zheng-Xin Liu, Xiaofei Qi, Nengkun Yu, Bei Zeng, and Duanlu Zhou. Physical origins of ruled surfaces on the reduced density matrices geometry. Science China Physics, Mechanics & Astronomy, 60(2):020311, Dec 2016.
- [35] Jianxin Chen, Zhengfeng Ji, Chi-Kwong Li, Yiu-Tung Poon, Yi Shen, Nengkun Yu, Bei Zeng, and Duanlu Zhou. Discontinuity of maximum entropy inference and quantum phase transitions. New Journal of Physics, 17(8):083019, 2015.
- [36] Rolf Schneider. Random hyperplanes meeting a convex body. Zeitschrift für Wahrschein-

- lichkeitstheorie und Verwandte Gebiete, 61(3):379-387, Sep 1982.
- [37] Michael A. Nielsen and Isaac L. Chuang. Quantum Computation and Quantum Information: 10th Anniversary Edition. Cambridge University Press, New York, NY, USA, 10th edition, 2011.
- [38] Jacob Biamonte, Peter Wittek, Nicola Pancotti, Patrick Rebentrost, Nathan Wiebe, and Seth Lloyd. Quantum machine learning. *Nature*, 549:195C–202, Sep 2017.
- [39] Maria Schuld and Francesco Petruccione. Quantum Machine Learning, pages 1034–1043.
 Springer US, Boston, MA, 2017.
- [40] N. Wiebe, A. Kapoor, and K. M. Svore. Quantum Deep Learning. ArXiv e-prints, December 2014.
- [41] D. Crawford, A. Levit, N. Ghadermarzy, J. S. Oberoi, and P. Ronagh. Reinforcement Learning Using Quantum Boltzmann Machines. *ArXiv e-prints*, December 2016.